Acceptor activation of Mg-doped GaN – Effects of N_2/O_2 vs N_2 as ambient gas during annealing

Ashutosh Kumar,[1,], Martin Berg[1], Qin Wang[2], Jun Uzuhashi[3], Tadakatsu Ohkubo[3], Michael Salter[2], and Peter Ramvall,[1,]**

[1]RISE Research Institutes of Sweden, Scheelevägen 17, SE-223 63 Lund, Sweden
[2]RISE Research Institutes of Sweden, Isafjordsgatan 22, SE-164 40 Kista, Sweden
[3]National Institute for Materials Science, Tsukuba 305-0047, Japan

* **Corresponding author(s):** ashutosh.kumar@ri.se, peter.ramvall@ri.se

ABSTRACT

Here, we investigate the effects of O_2:N_2 (1:1) as ambient gas as compared with pure N_2 during activation annealing of Mg as p-type doping in GaN layers grown by MOCVD. The purpose is to understand the impact of O_2 on the resulting free hole concentration and hole mobility using SIMS, XRD, STEM, AFM and Hall effect measurements. Even though the presence of O_2 in the ambient gas during annealing is very effective in reducing the H level of the Mg-doped GaN layers, the maximum achievable hole concentration and mobility is still higher with pure N_2. The differences are explained by an in-diffusion of O to the GaN layer acting as n-dopant and thus giving rise to a compensation effect. The Mg-H complexes at substitutional (Mg_{Ga}), i.e., the electrically active acceptor sites that provide free holes, are preferentially activated by annealing with N_2 only as ambient gas, while annealing with O_2:N_2 (1:1) also dissociates electrically inactive Mg-H complexes resulting in much less residual H. At the lower growth pressure of 150 mbar compared to higher growth pressure of 300 mbar, an increasing carbon incorporation leads to a compensation effect drastically reducing the free hole concentration while the mobility is unaffected.

I. INTRODUCTION

It has been more than 30 years since the ground-breaking discovery of p-doping GaN that opened for the development of blue and white LEDs and low-power displays in smartphones that changed our way of life.[1-4] A special feature of the discovery was that the dopant, Mg in this case, needs to be activated in order to produce holes needed for the p-type conduction. The activation can occur by low-energy electron beam irradiation [1] or a heat treatment such as rapid thermal processing (RTP).[2,3] The discovery opened for the realization of a GaN-based p-n junction, an important part in many electronic devices, and thus, the achievement of a precise control of p-type conductivity is considered as a crucial issue in devices such as vertical p-n diodes for high-power applications and blue light emitting diodes for lighting applications. Mg substitutional to Ga is the preferred acceptor for p-type doping of GaN due to its relatively low activation energy, with reported values between 155 and 230 meV [5-8] and commonly used

in p-GaN fabrication by metal-organic chemical vapor deposition (MOCVD).

However, still the realization of high hole concentrations in p-type GaN films is one of the limiting factors for obtaining highly efficient GaN-based optoelectronic devices. It is now well-accepted that hydrogen molecules from NH_3 in MOCVD form inactive bonds with Mg atoms, and these bonds need to be dissociated for Mg activation. Rapid thermal processing (RTP) has proven to be the most promising way to achieve this Mg activation in Mg-doped GaN layer. For example, by application of RTP in a N_2 atmosphere at temperatures above 700°C, p-GaN with resistivity, hole concentration and hole mobility of 2 Ωcm, $3\times10^{17}cm^{-3}$ and 10 $cm^2V^{-1}s^{-1}$, respectively, were realized early.[2] In addition to temperature, the ambient gas during activation of the Mg-dopant has an important role and it was found that by adding O_2 a higher hole concentration was obtained for a given activation temperature.[9] By applying secondary ion mass spectroscopy (SIMS) after activation annealing the H level was found to be clearly lower when 10% O_2 was added to the N_2 ambient during activation. The samples with less H also showed a lower resistivity at optimized activation time; for longer times, the resistivity was observed to increase, which was attributed to a compensation effect by in-diffusion of oxygen.[9] Similar results were obtained by activation in pure O_2.[10] Kuo *et al.* found that with O_2 present during activation annealing, hole concentrations of $3\times10^{17}cm^{-3}$ may be obtained already at 400 °C.[11] The finding that less residual H after activation annealing improves the electrical properties is in line with that dissociation of the Mg-H complex is the key process for activation of p-doping by Mg in GaN.[3,12-14]. Considering different temperatures, ambient gases, annealing times etc, it can be said that the processes involved to achieve p-type conduction in GaN are still not completely understood but are to a large degree based on empirical observations and know-how.

Other important factors that may affect the result of p-doping GaN with Mg are dislocations, defects, and hillocks, and on the substrate type used.[15,16] The presence of another epitaxial layer on the p-GaN layer can also severely affect the doping activation efficiency by to some degree hindering the H from out-diffusing through the surface.[14] It is also known that growth of an additional GaN layer on top of an activated p-GaN layer may re-passivate the Mg doping of the underlying GaN layer.[14] Recently, it was found that O_2 during annealing enhances the diffusion rate of Mg in the layer.[17] Furthermore, annealing in pure or partial O_2 has also been found effective in improving ohmic contacts on p-type GaN.[18,19]

II. EXPERIMENTAL

Epitaxial growths were performed using an Aixtron 7×2” close-coupled showerhead (CCS) MOCVD tool. Purified ammonia (NH_3), trimethylgallium (TMGa) and biscyclopentadienyl magnesium (Cp_2Mg) were used as precursors for nitrogen, gallium, and magnesium, respectively. Epison 4 in-line gas concentration monitors were used for precursor concentration control. Purified hydrogen (H_2) with a dew point less than -110 ^oC was used as carrier gas.

Mg-doped p-GaN layers were grown on 2″ c-plane (0001) sapphire substrates. First a standard 3-µm-thick unintentionally-doped buffer layer was epitaxially grown on the sapphire substrate, followed by a 0.5-µm-thick semi-insulating (SI) GaN layer by carbon auto-doping, and a 0.5-µm-thick Mg-doped GaN layer. The SI GaN layer was intentionally grown to electrically isolate the top Mg-doped layer from the buffer layer which is crucial in Hall measurements to minimize the contribution in carrier densities in top-layer from the buffer layer.

In this study, two different GaN growth conditions of the Mg-doped layer were used. In both cases the layers were grown at 995 °C, as measured on the wafer by the Argus top-temperature controller (TTC). The V/III-ratio in the gas phase was 1500 and the growth pressures were 300 mbar and 150 mbar that resulted in growth rates of about 1.2 µm/hour and 3.0 µm/hour, respectively. In order to keep the NH_3 partial pressure constant at the lower growth pressure, the supplied amount of TMGa and NH_3 were doubled. The total carrier gas flow was kept constant; thus, a thinner growth surface diffusion layer (boundary layer) may be expected at the lower pressure with higher carrier gas velocity. The substantially higher growth rate at 150 mbar is most likely caused by the doubling of the TMGa flow together with the thinner diffusion layer.

The Mg doping levels targeted at 300 mbar growth pressure were 1×10^{19} cm^{-3}, 4×10^{19} cm^{-3}, and 8×10^{19} cm^{-3} that corresponds to growth with 1.3%, 2.6%, and 4.0% Cp_2Mg taken as the molar flow relation between Cp_2Mg and TMGa in the gas phase. At 150 mbar growth pressure the targeted levels were 1×10^{19} cm^{-3} and 4×10^{19} cm^{-3}, corresponding to growth with 0.3% and 1.3% Cp_2Mg. The Mg incorporations were confirmed by SIMS. No in-situ Mg-doping activation process in the MOCVD growth chamber was applied.

Atomic force microscopy (AFM) characterization was done in tapping mode by a Bruker Dimension Icon on 3.0×3.0 μm^2 sample surface area. The analysis of the captured AFM images was done by Nanoscope software. X-ray diffraction (XRD) characterization was done by a Bruker D8 Discovery equipped with PathFinder detector with variable slit and three bounce Ge (220) crystal. In order to improve the precision of the characterization, AFM and XRD were performed at several points over the 2” wafer and the average of the measured values were taken.

Rapid thermal processing (RTP) was performed in an RTP-1200-100 from UniTemp GmbH. Wafers were ramped to a target temperature of 900 °C at 80 °C/second in N_2/O_2 ambient with an overshoot of less than 10 °C, stay for 5 minutes at 900 °C in N_2/O_2 ambient, followed by cooling only in N_2 ambient. Before any RTP involving Mg-doped GaN samples the tool was first tested by RTP of a dummy wafer at the same condition as was to be used for the Mg activation. SIMS was performed by a Cameca double-focusing magnetic sector tool. Approximate SIMS detection limits/background levels were; Mg: 3×10^{16} cm^{-3}, H: 2×10^{17} cm^{-3}, C: < 1×10^{17} cm^{-3}, O: 1×10^{17} cm^{-3}.

Microstructural investigations were carried out by cross-sectional low-angle annular dark-field (LAADF-) scanning transmission electron microscopy (STEM) observation by using Thermo Fisher

Scientific Titan G2 80–200 at 200 kV. STEM specimens were prepared by the standard lift-out method using a focused ion beam (FIB) with a scanning electron microscopy (SEM) system, Thermo Fisher Scientific Helios 5UX.[20]

Electrical measurements were performed in the van der Pauw geometry on square samples manufactured by thermal evaporation of Ni/Au (20/100 nm) as ohmic contacts followed by cutting the 2" wafers in 3×3 mm^2 squares, thus forming contacts in the sample corners. The contacts were not annealed, but for the GaN growth with 0.3% and 1.3% Cp_2Mg an approximately 25-nm-thick Mg-doped GaN top layer with 2.6% Cp_2Mg was grown to improve the ohmic contacts. The samples were then characterized by van der Pauw and Hall effect measurements to determine the hole concentrations (p), hole mobilities (μ), and resistivity (ρ). For the measurements, the sourcing was done using Keithley 2602 SMU, with the voltage measurements being performed using a Keithley 6514 electrometer. The magnetic field was applied using a Bouhnik AF14108 electromagnet and power supply system, controlled by magnetic field probing using a Lakeshore 475D Gaussmeter. The measurements were performed at different drive current levels and result was compared in order to ensure that the result was not affected by heating or leakage etc. induced by too high current or voltage levels.

III. RESULTS

After MOCVD growth the wafers were investigated by AFM and XRD. Fig. 1 displays the results of the AFM investigation on the wafers grown at 300 mbar. Typically, the surface step heights increase with increasing Mg concentration, presumably due to step bunching. Mg concentrations up to about 4×10^{19} cm^{-3} has no major effect on the surface roughness. The average (R_a) and RMS (R_q) roughness for 1×, 4×, and 8×10^{19} cm^{-3} Mg were R_q ~ 0.2 nm, R_a ~ 0.15 nm, R_q ~ 0.35 nm, R_a ~ 0.25 nm, R_q ~ 1.25 nm, R_a ~ 0.80 nm, respectively. The roughness values for 1×10^{19} cm^{-3} Mg are similar to those of undoped epitaxial GaN layers (R_q ~ 0.17 nm, R_a ~ 0.13 nm) as shown in the supplementary information. At 8×10^{19} cm^{-3} Mg the as-grown surface is rougher and optical microscopy revealed hillocks on the epitaxial surface.

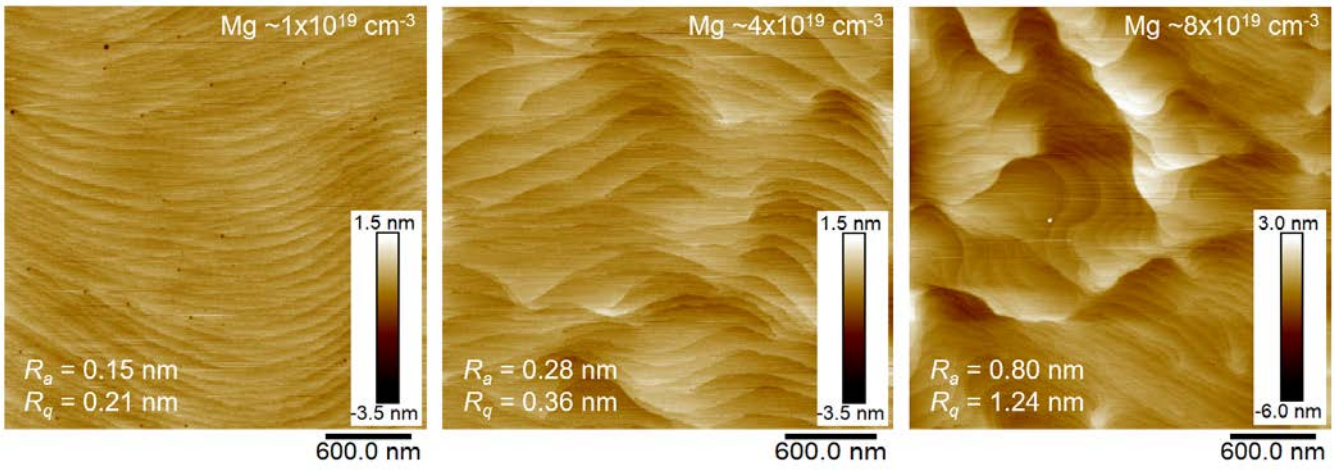

FIG 1. AFM micrographs of p-GaN surfaces grown at 300 mbar with 1×, 4×, and 8×10^{19} cm^{-3} Mg. The roughening of the surfaces most likely occurs by step-bunching induced by the increasing amount of Mg.

Another effect of increasing Mg-doping appears to be fewer threading dislocations reaching the surface. The density of threading dislocations, observed as small black dots, for 1×10^{19} cm^{-3} Mg is around $3\text{-}5\times10^{8}$ cm^{-2}, similar to what is commonly observed for GaN grown on sapphire substrates.

Structural properties of the Mg-doped GaN layers were examined with XRD-based rocking curve measurements as presented in Fig. 2. In such measurement, the detector is set at the Bragg angle corresponding to GaN and sample is tilted. The width of the peak provides information about the crystalline quality of the GaN layer. For GaN growth without Mg-doping, the (0002) peak width is usually around 300 arcsec confirming good crystalline quality of the layer. The resulting full width at half maximum (FWHM) and XRD peak positions for Mg incorporations as determined by SIMS at 1×, 4×, and 8×10^{19} cm^{-3}, were 293.4 and 17.52, 310.7 and 17.60, and 332.9 and 17.01, arcsec and degrees, respectively. In comparison to the undoped GaN layer where width of the XRD (0002) rocking curve diffraction peak was found to be ~ 293.3 arcsec (see supplementary information), very small or no increase of peak width was observed for the smallest amounts of Mg. This suggests that doping with about 1×10^{19} cm^{-3} Mg does not lead to degradation of the crystalline quality of GaN layer. However, as Mg incorporation is increased to 4×10^{19} cm^{-3} and 8×10^{19} cm^{-3}, the width of the (0002) peak increases. This may be attributed to the formation of Mg-induced defects like clusters or pyramids as reported earlier.[16,21,22] The (0002) peak position is significantly shifted for 8×10^{19} cm^{-3} Mg, suggesting expansion of the GaN lattice which may be caused by incorporation of Mg at interstitial lattice positions leading to strain.

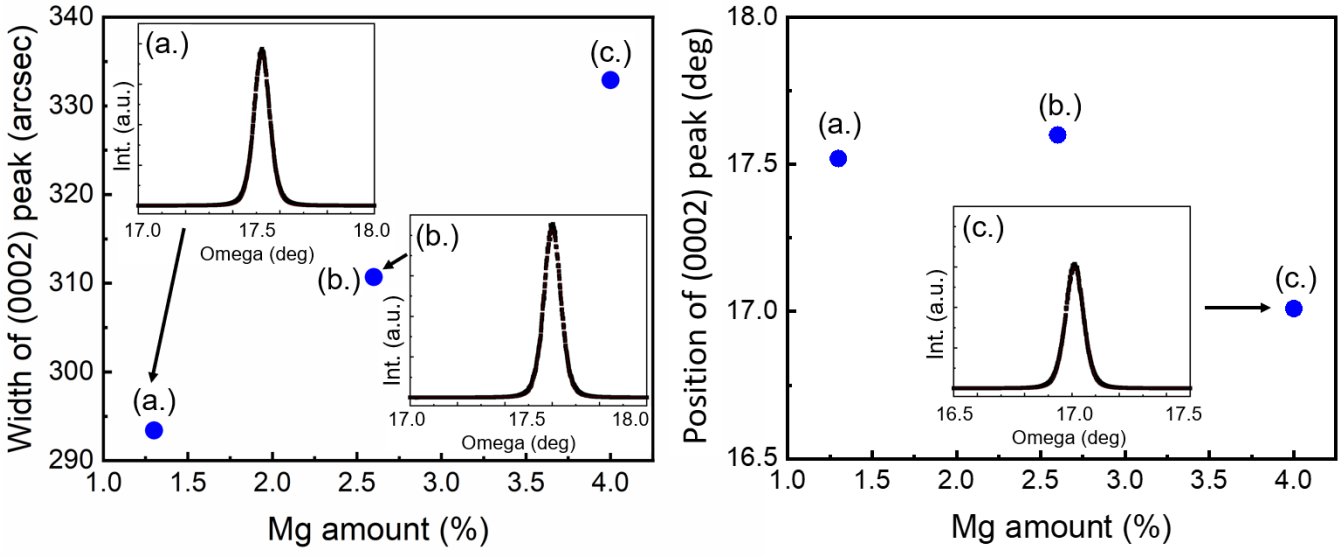

FIG 2. XRD of (0002) symmetrical plane of p-GaN grown at 300 mbar with varying amount of Cp_2Mg during growth, (a. 1.3%), (b. 2.6%), and (c. 4.0%), obtained through rocking curve measurements. A width of less than 300 arcsec at 1×10^{19} cm^{-3} Mg suggests a good quality of the grown Mg-doped GaN layers. The FWHM and XRD peak positions for 1.3%, 2.6% and 4.0% Mg, were 293.4 and 17.52, 310.7 and 17.60, and 332.9 and 17.01, arcsec and degrees, respectively. As expected, the width was found to increase with increasing amount of Mg due to Mg-induced structural deformations, most likely Mg at interstitial positions that also appears

to expand the lattice and move the XRD peak position to smaller angle (from about 17.5 to 17.0 degrees).

To activate the Mg-doping, the wafers were cut to quarters and RTP was carried out at different temperatures, ranging between 700 ^{o}C and 975 ^{o}C under N_2 and O_2:N_2 (1:1) gas mixtures. The general trend observed is that by adding O_2 during the activation annealing the temperature where the activation commences appears to be lower.[9-11] However, to achieve saturation i.e., minimize the resistivity, relatively high RTP temperature is required, whereas only a small difference is expected between RTP ambient gas of N_2 and O_2:N_2 (1:1).[9-10] By applying SIMS analysis for some different RTP temperatures, it was found that RTP for 5 minutes at temperatures lower or higher than 900 ^{o}C resulted in activation saturation (SIMS spectra for 850 °C and 975 °C are shown in supplementary information), as judged by the reduction of the H level, of the Mg doping levels in this study.

The result of the SIMS investigation of RTP for 5 minutes at 900 ^{o}C on the wafers grown at 300 mbar MOCVD reactor pressure is shown in Fig. 3, where a test matrix with the amount of Cp_2Mg in the gas-phase during growth in relation to TMGa 1.3%, 2.6%, and 4.0%, for as grown, N_2, and O_2:N_2 (1:1) RTP processed Mg-doped GaN is presented. The onset of the Mg doping appears to be fairly slow, especially at the lower concentrations. The reason is believed to be that before steady-state incorporation can start ~ 0.3 monolayers of Mg are needed at the growth surface.[13] The most prominent difference between the RTP ambients can be observed for the H level of the topmost 0.5-μm-thick Mg-doped GaN. Before annealing, H follows the Mg level up to around 4×10^{19} cm^{-3} where it appears to saturate. Depending on the gas mixture a striking differences on the impact of H level is evident; O_2:N_2 (1:1) is by far superior in suppressing H. It has been suggested that O_2 contributes to a more efficient hydrogen removal by forming H_2O molecules on the GaN surface.[19] In the case of N_2, the reduction of the H level is limited to about 1×10^{19} cm^{-3} regardless of the Mg-doping level. Another result of RTP, similar regardless of ambient gas, is that the H level of the 0.5-μm-thick SI GaN is reduced down to the background level of ~ 2×10^{17} cm^{-3}.

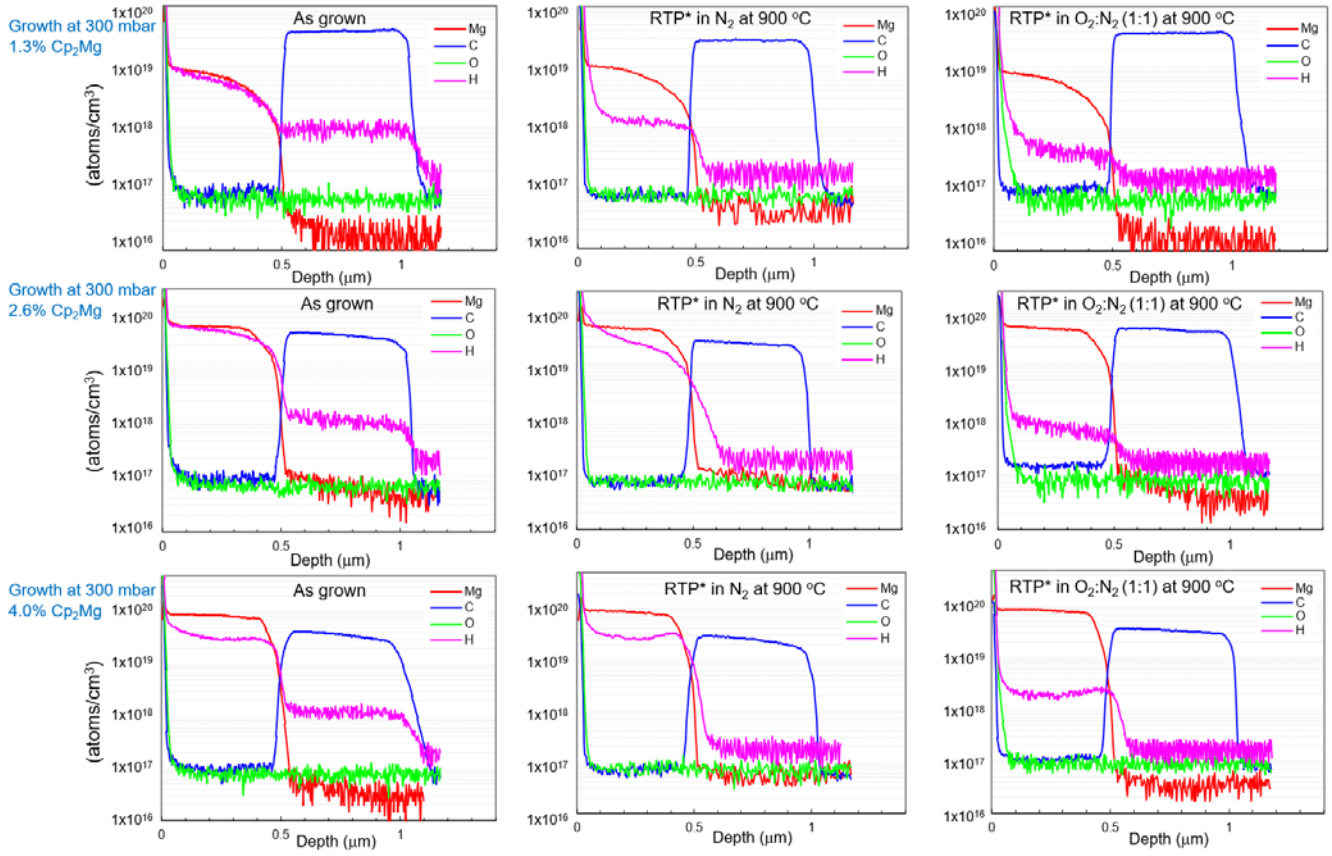

FIG 3. SIMS spectra of Mg-doped GaN layers grown at 300 mbar before and after activation annealing at 900 °C. The rows of SIMS spectra represent the amount of Cp_2Mg in the gas-phase during growth in relation to TMGa (1.3%, 2.6%, and 4.0%) and the columns for as grown, RTP processed in N_2, and O_2:N_2 (1:1) ambient gas. Before annealing H follows the Mg level up to around 4×10^{19} cm^{-3}.

The SIMS investigation of the p-GaN layer grown at 150 mbar is displayed in Fig. 4. Two p-GaN growths at 150 mbar with 0.3% and 1.3% Cp_2Mg have been characterized. At these relatively low Mg-doping levels the surface roughness and XRD rocking curve peak width is approximately similar to undoped GaN ~ 293.3 arcsec as shown in the supplementary information. Comparing the Mg incorporation for growth at 150 mbar with 300 mbar reactor pressure the incorporation appears to have increased four-fold; 1.3% Cp_2Mg in the gas-phase gave 4×10^{19} cm^{-3} Mg in the solid phase and 0.3% Cp_2Mg gave 1×10^{19} cm^{-3} Mg, respectively. The reason for the increased incorporation might be less parasitic pre-reactions of Cp_2Mg in the gas phase at the lower growth pressure, also the fact that Cp_2Mg is a relatively large molecule and may diffuse easier through the thinner boundary layer at 150 mbar may play a role. Judging from the reduction of the H-level, the activation by RTP in the case of N_2 ambient gas appears to be substantially more effective on the GaN layer with 4×10^{19} cm^{-3} Mg grown at 150 mbar compared to 300 mbar in Fig. 3. This observation suggests that the Mg might be incorporated differently for growth at 150 mbar than 300 mbar.

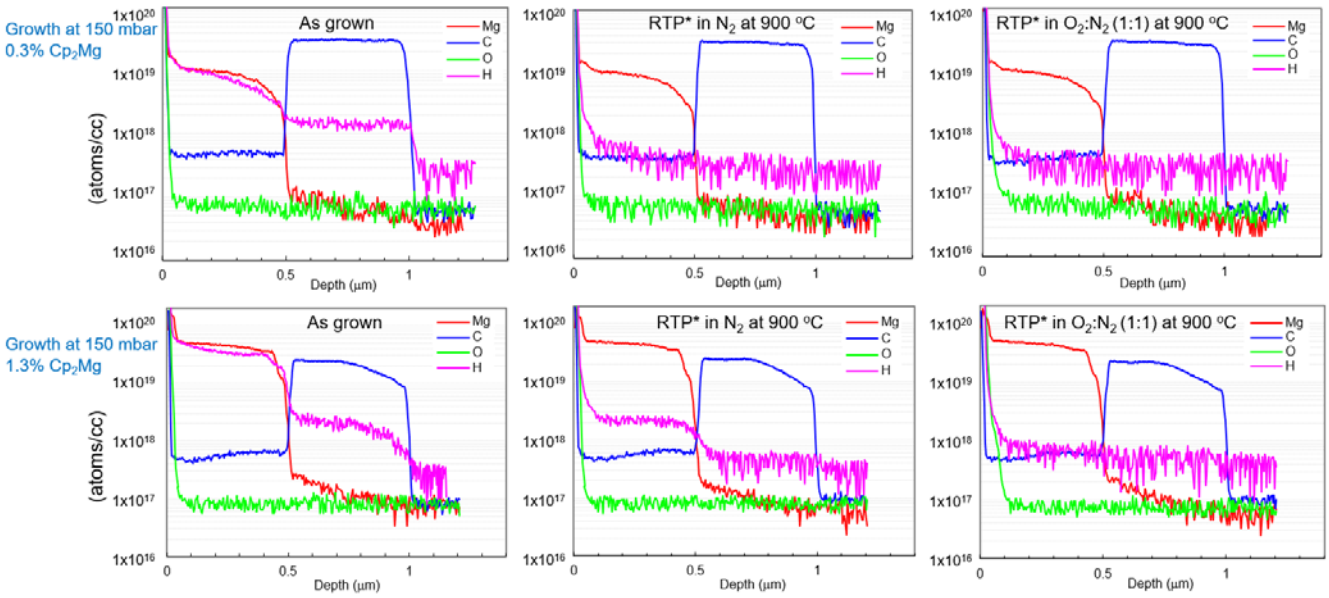

FIG 4. SIMS spectra of Mg-doped GaN layers grown at 150 mbar before and after activation annealing at 900 °C. The upper and lower rows are for p-GaN grown at 150 mbar with 0.3% and 1.3% Cp_2Mg, respectively. The columns represent as grown, RTP processed in N_2, and O_2:N_2 (1:1) ambient gas. Before annealing H follows the Mg level after RTP the H levels are substantially lower. It is clear that the Mg incorporation is substantially larger at 150 mbar growth pressure where 1.3% Cp_2Mg results in about 4×10^{19} cm^{-3}; a fourfold increase compared with p-GaN grown at 300 mbar shown in Fig. 3. For growth at 150 mbar an Mg level of 1×10^{19} cm^{-3} can be obtained with 0.3% Cp_2Mg in the gas phase. Another important observation is that the carbon level in the Mg-doped layer is substantially higher for growth at 150 mbar reactor pressure than at 300 mbar in Fig. 3.

Electrical characterization on all samples annealed at 900 °C was performed by Hall in van der Pauw configuration. A uniform sheet resistance was measured from the four possible directions. Typical data for RTP at 900 °C in O_2:N_2 (1:1) for Mg-doped GaN grown at 300 mbar reactor pressure is shown in Fig. 5. Except for the highest Mg doping level, the Hall mobilities are typically around 8-9 $cm^2V^{-1}s^{-1}$ and the hole concentrations are $4\text{-}5\times10^{17}$ cm^{-3}, as calculated from the sheet concentration and the 500-nm-film thickness at the corresponding sourcing current in the $-1\ \text{T} \le B \le 1\ \text{T}$ magnetic field range.

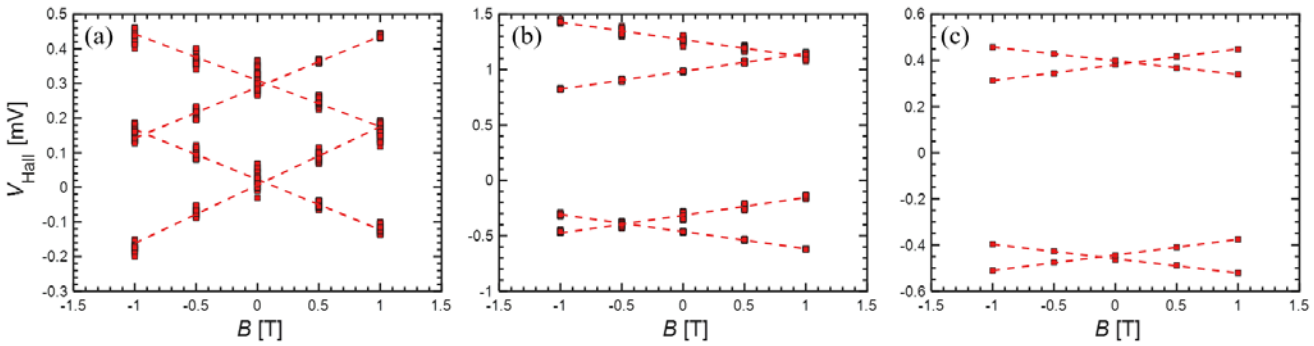

FIG 5. Room temperature Hall characterization of the three samples corresponding to the Cp_2Mg/TMGa

ratios 1.3% (a), 2.6% (b), 4% (c) annealed at 900 °C in O_2:N_2 (1:1) using the van der Pauw Hall method. Hole mobilities, μ, of 8.0, 8.3, 6.4 $cm^2V^{-1}s^{-1}$ and hole concentrations, p, of 4.2×10^{17}, 4.0×10^{17}, and 2.0×10^{17} cm^{-3} are extracted for the three samples respectively with p being calculated from the sheet concentration using the 500-nm-film thickness. Sourcing currents of 5 µA was applied for (a) and (b), and 1 µA for (c). The data was confirmed by lower sourcing currents to limit the possible injection into underlying GaN layers. The, in some cases, observed asymmetric V_{Hall}-B trends are attributed to sample size non-uniformities.

To further understand the correlation between electrical and structural properties, we have carried out scanning transmission electron microscopy (STEM) on all three samples with Mg~ 1×10^{19} cm^{-3}, 4×10^{19} cm^{-3} and 8×10^{19} cm^{-3} annealed under N_2 ambient, as shown in Fig. 6. Imaging was performed under low-angle annular dark field (LAADF) condition.[23-26]

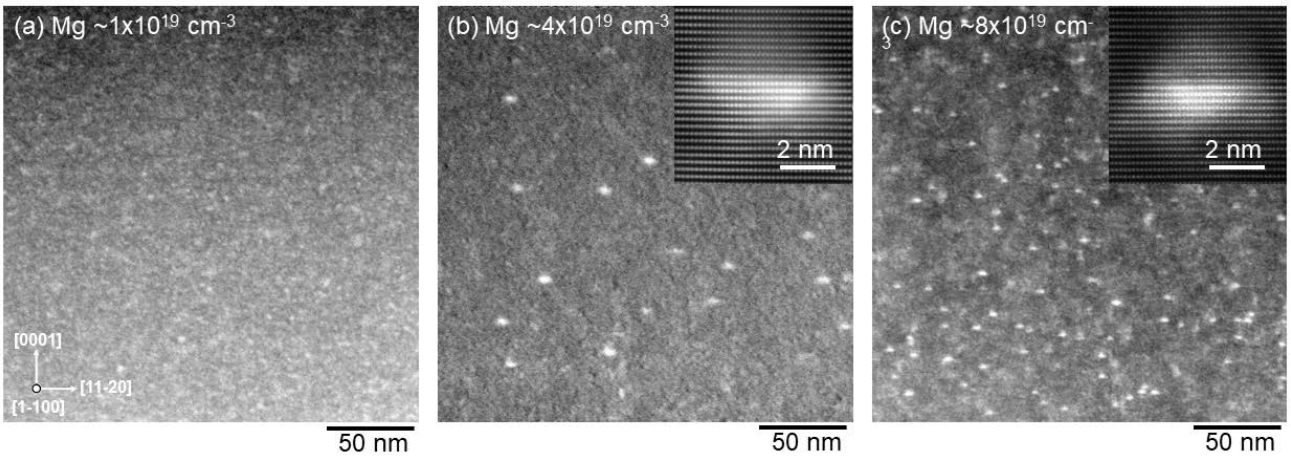

FIG 6. Cross-sectional LAADF-STEM images of 1×, 4×, and 8×10^{19} cm^{-3} Mg-doped GaN. Pyramidal defects were observed in 4× and 8×1019 cm-3 samples, but not in 1×10^{19} cm^{-3}. Each inset in 4× and 8×10^{19} cm^{-3} shows a high-magnification STEM image of pyramidal defects.

IV. DISCUSSION

The measured hole mobility and hole concentration of all samples annealed at 900 °C are presented in Table I. The general trend appears to be that RTP at 900 °C in N_2 results in slightly higher mobility and hole concentration leading to a substantially lower resistivity. The samples with 8×10^{19} cm^{-3} Mg show lower hole concentrations and mobility, possibly due to the formation of compensating defects with donor-like behavior involving a complex,[21] for example, Mg_2–V_N–H, where V_N is a nitrogen vacancy.[27] Such a complex would be a neutral defect during growth but would become a donor, which may cause a compensation effect once the hydrogen was removed by the activation process. At high Mg concentrations the normally deep donor Mg_{Ga}–V_N may contribute to compensation.[28,29]

	RTP in N_2 at 900 °C	RTP in O_2:N_2 1:1 at 900 °C

Mg ~ $1x10^{19}$ cm^{-3} Growth at 150 mbar Cp_2Mg = 0.3%	p = $0.87x10^{17}$ cm^{-3} μ = 18.6 $cm^2V^{-1}s^{-1}$ ρ = 3.8 Ohm-cm	Not measurable
Mg ~ $4x10^{19}$ cm^{-3} Growth at 150 mbar Cp_2Mg = 1.3%	p = $1.12x10^{17}$ cm^{-3} μ = 10.0 $cm^2V^{-1}s^{-1}$ ρ = 5.6 Ohm-cm	p = $1.03x10^{17}$ cm^{-3} μ = 9.2 $cm^2V^{-1}s^{-1}$ ρ = 6.6 Ohm-cm
Mg ~ $1x10^{19}$ cm^{-3} Growth at 300 mbar Cp_2Mg = 1.3 %	p = $4.9x10^{17}$ cm^{-3} μ = 9.3 $cm^2V^{-1}s^{-1}$ ρ = 1.37 Ohm-cm	p = $4.2x10^{17}$ cm^{-3} μ = 8.0 $cm^2V^{-1}s^{-1}$ ρ = 1.86 Ohm-cm
Mg ~ $4x10^{19}$ cm^{-3} Growth at 300 mbar Cp_2Mg = 2.6%	p = $4.5x10^{17}$ cm^{-3} μ = 9.1 $cm^2V^{-1}s^{-1}$ ρ = 1.53 Ohm-cm	p = $4.0x10^{17}$ cm^{-3} μ = 8.3 $cm^2V^{-1}s^{-1}$ ρ = 1.91 Ohm-cm
Mg ~ $8x10^{19}$ cm^{-3} Growth at 300 mbar Cp_2Mg = 4.0%	p = $3.8x10^{17}$ cm^{-3} μ = 7.8 $cm^2V^{-1}s^{-1}$ ρ = 2.1 Ohm-cm	p = $2.0x10^{17}$ cm^{-3} μ = 6.4 $cm^2V^{-1}s^{-1}$ ρ = 5.0 Ohm-cm

TABLE I. Hole concentration, hole mobility, and resistivity at room temperature of Mg-doped GaN samples activated by RTP at 900 °C in N_2 and O_2:N_2 (1:1). The values are determined by Hall characterization in the van der Pauw configuration.

The Hall data indicates that even though SIMS characterization clearly shows a significant lowering the of H level by adding O_2 during RTP it has a small effect on the electrical characteristics. This result is surprising since the dissociation of the Mg-H complex is considered to be the key process for activation of p-doping by Mg in GaN.[3,12-14] However, it has also been suggested that H combines with Mg to form two different types of Mg-H complexes: one metastable, presumably with Mg substitutional to Ga, leading to the Mg acceptor after annealing and one dominating at high Mg levels being stable and electrically inactive.[13] The correlation between the amount of incorporated Mg and free hole concentration is further explained by by STEM where pyramidal defects were observed in the samples with Mg ~ 4×10^{19} cm^{-3} and Mg ~ 8×10^{19} cm^{-3} as shown in Fig. 6. These defects were not observed in sample with lowest amount of Mg ~ 1×10^{19} cm^{-3}. The number density of these pyramidal defects is found to be significantly higher in sample with Mg ~ 8×10^{19} cm^{-3} which explains the lowest hole concentration in this sample in comparison to other samples. Kumar *et al.*[16,30] and other authors[31,32] reported that these defects provide segregation sites for Mg and may act as the compensating centers which may lead to a decrease in free hole concentration.

Considering hole concentration of about 1×10^{18} cm^{-3} for Mg-doped GaN as measured by Hall effect at room temperature with a maximum at an Mg-doping level at around 2-3$\times10^{19}$ cm^{-3} [33] and that about 10% of the holes are ionized at room temperature,[21] about 1×10^{19} cm^{-3} substitutional Mg dopants need to activate. The measured maximum hole concentration in this work of 4-5$\times10^{17}$ cm^{-3} translates to about 4-5$\times10^{18}$ cm^{-3} activated Mg-dopants on substitutional Mg sites. Comparison of the SIMS results for 1×10^{19} cm^{-3} Mg (1.3%) grown at 300 mbar before and after RTP in N_2 in Fig. 3 indicates a lowering of

the H levels of about 4-5×10^{18} cm^{-3} which commensurate with the measured hole concentration of about 4-5×10^{17} cm^{-3}. The same is true for the other samples grown at 300 mbar after RTP in N_2, 4×10^{19} cm^{-3} Mg (2.6%) and 8×10^{19} cm^{-3} Mg (4.0%), albeit less clear because of the higher Mg content. In the case of RTP in O_2:N_2 (1:1) the reductions of the H levels of all samples grown at 300 mbar are substantially larger. This finding suggests that only the Mg-H complexes at substitutional (Mg_{Ga}) electrically active acceptor sites are dissociated by RTP with N_2 as ambient gas, while RTP with O_2:N_2 (1:1) also dissociates electrically inactive Mg-H complexes. Thus, the residual H measured by SIMS after activation annealing with N_2 may provide a representative measure of the resulting hole concentration.

With reference to Table I, for growth at 150 mbar reactor pressure the relation between the Mg incorporation in relation to the resulting hole concentration after RTP is radically different. Both the sample with 1×10^{19} cm^{-3} Mg and 4×10^{19} cm^{-3} Mg, in spite of having comparably lower H levels after RTP at 900 °C in N_2, showed hole concentrations of only about 1×10^{17} cm^{-3}, a lot less than may have been expected from the results at 300 mbar. A possible reason for the low hole concentration may be the larger amount of residual carbon in the Mg-doped layer grown at 150 mbar, as seen in Fig. 4 compared with growth at 300 mbar in Fig. 3. A larger amount of residual carbon is commonly observed at lower GaN growth pressures.[34] The excess carbon may lead to a compensation effect [35-37] making the GaN material become semi-insulating [38] that may be the case for layer grown at 150 mbar with 0.3% Cp_2Mg that was not measurable after RTP in O_2:N_2 (1:1). The increase of C by about 4×10^{17} cm^{-3} at 150 mbar corresponds fairly well to the loss of holes compared to the p-GaN layers with corresponding Mg levels grown at 300 mbar.

However, still the activation annealing in N_2 for the layers grown at 150 mbar appears to be more effective than N_2 annealing for samples grown at 300 mbar. This is especially clear when comparing the H level for SIMS of the 300 mbar for Mg = 4×10^{19} cm^{-3} (2.6%) sample in Fig. 3. with the H level of the 150 mbar Mg = 4×10^{19} cm^{-3} (1.3%) sample in Fig. 4. Applying the previous result that N_2 primarily activates Mg-H complexes on electrically active sites substitutional to Ga growth at 150 mbar may be more favorable than 300 mbar in order to obtain a high hole concentration provided the carbon impurity is kept low.

As can be seen in Table I. the layers activated by RTP at 900 °C in O_2:N_2 (1:1) show a slightly lower hole concentration compared to those in pure N_2. A possible explanation for the observed effect may be that oxygen in GaN forms a donor.[39-41] By applying SIMS with higher sensitivity (~ 3-4×10^{15} atoms/cc), as shown in the supplementary information, it appears that there is an interdiffusion of O to a level of about 5×10^{16} cm^{-3} down to a depth of about 250 nm of the 1×10^{19} cm^{-3} Mg-doped GaN layer and basically throughout the entire Mg-doped layer of the sample with 4×10^{19} cm^{-3} Mg. Oxygen is known to diffuse into GaN at temperatures similar to the RTP in this work.[9,42,43] Thus, the lower hole concentration might be attributed to compensation by n-type doping from O. The slightly lower mobility, as seen in Table I. for RTP activation in O_2:N_2 (1:1) as ambient gas, may also be explained by the higher impurity level from

O in-diffusion to the p-GaN layer.

V. CONCLUSIONS

The reduction of the residual H level of an Mg-doped GaN layer is substantially more effective in the presence of O_2 during RTP, still the hole concentration and hole mobility were found to be higher for activation annealing in pure N_2. Since only the Mg-H complexes at substitutional (Mg_{Ga}) electrically active acceptor sites will provide free holes our findings suggest that these sites are preferentially dissociated by RTP with N_2 as ambient gas, while RTP with O_2:N_2 (1:1) also dissociates electrically inactive Mg-H complexes. Thus, the residual H level in relation to the Mg level after activation annealing with N_2 only may provide a representative measure of the resulting free hole concentration of the Mg-doped GaN layer. As revealed by STEM, an increase in incorporated Mg leads to the increase in number density of pyramidal defects, and these pyramidal defects may act as the compensating centres which explains the lowest hole concentration in sample with highest Mg in present work.

Depending on the amount of Mg incorporated in the GaN layer, the MOCVD reactor pressure during growth, and the ambient gas during Mg activation annealing, different types of compensation mechanisms are dominating. At the highest Mg incorporation, in this work about 8×10^{19} cm^{-3}, compensation may occur by the formation of compensating defects involving a complex such as Mg_2–V_N–H with donor-like behavior. At the lower growth pressure, 150 mbar, the increasing carbon incorporation leads to a compensation effect that may ultimately making the GaN material become semi-insulating. With O_2:N_2 (1:1) as ambient gas during activation annealing the hole concentration and mobility were found to be lower than with N_2 only. The effect may be explained by the incorporation of O as n-doping in GaN leading to compensation.

ACKNOWLEDGMENTS

This project has received funding from the ECSEL Joint Undertaking (JU) under grant agreement No 826392. The JU receives support from the European Union's Horizon 2020 research and innovation program and Austria, Belgium, Germany, Italy, Slovakia, Spain, Sweden, Norway, and Switzerland.

AUTHOR DECLARATIONS

Conflict of Interest

The authors have no conflicts of interest.

Author Contributions

Ashutosh Kumar: Formal analysis (equal); Investigation (equal); Methodology (equal); Visualization (equal); Writing – review & editing (equal) **Martin Berg**: Formal analysis (equal); Investigation (equal); Methodology (equal); Visualization (equal); Writing – review & editing (equal); Data Curation (lead)**;** **Qin Wang:** Conceptualization (equal); Validation (lead); Supervision (equal); **Michael Salter:**

Conceptualization (equal): Funding acquisition (lead); Supervision (equal); Project administration (lead); **Peter Ramvall:** Formal analysis (equal); Investigation (equal); Methodology (equal); Visualization (equal); Writing – original draft (lead); Resources (lead);

REFERENCES

[1] H. Amano, M. Kito, K. Hiramatsu, and I. Akasaki, "P-Type Conduction in Mg-Doped GaN Treated with Low-Energy Electron Beam Irradiation (LEEBI)" Jpn. J. Appl. Phys. **28**, L2112 (1989). https://doi.org/10.1143/JJAP.28.L2112

[2] S. Nakamura, T. Mukai, M. Senoh, and N. Iwasa, "Thermal Annealing Effects on P-Type Mg-Doped GaN Films" Jpn. J. Appl. Phys. **31**, L139 (1992). https://doi.org/10.1143/JJAP.31.L139

[3] S. Nakamura, N. Iwasa, M. Senoh, and T. Mukai, "Hole Compensation Mechanism of P-Type GaN Films" Jpn. J. Appl. Phys. **31**, 1258 (1992). https://doi.org/10.1143/JJAP.31.1258

[4] S. Nakamura, T. Mukai, M. Senoh, "Candela-class high-brightness InGaN/AlGaN double-heterostructure blue-light-emitting diodes" Appl. Phys. Lett. **64**, 1687 (1994). https://doi.org/10.1063/1.111832

[5] I. Akasaki, H. Amano, M. Kito, and K. Hiramatsu, "Photoluminescence of Mg-doped p-type GaN and electroluminescence of GaN p-n junction LED" J. Lumin. **48–49**, 666 (1991). https://doi.org/10.1016/0022-2313(91)90215-H

[6] S. Fischer, C. Wetzel, E. E. Haller, and B. K. Meyer, "On p-type doping in GaN—acceptor binding energies" Appl. Phys. Lett. **67**, 1298 (1995). https://doi.org/10.1063/1.114403

[7] W. Götz, N. M. Johnson, J. Walker, D. P. Bour, and R. A. Street, "Activation of acceptors in Mg-doped GaN grown by metalorganic chemical vapor deposition" Appl. Phys. Lett. **68**, 667 (1996). https://doi.org/10.1063/1.116503

[8] W. Kim, A. Salvador, A. E. Botchkarev, O. Aktas, S. N. Mohammad, and H. Morcoç, "Mg-doped p-type GaN grown by reactive molecular beam epitaxy" Appl. Phys. Lett. **69**, 559 (1996). https://doi.org/10.1063/1.117786

[9] B. A. Hull, S. E. Mohney, H. S. Venugopalan, and J. C. Ramer, "Influence of oxygen on the activation of p-type GaN" Appl. Phys. Lett. **76**, 2271 (2000). https://doi.org/10.1063/1.126318

[10] T.-C. Wen, S.-C. Lee, W.-I. Lee, T.-Y. Chen, S.-H. Chan, and J.-S. Tsang, "Activation of p-Type GaN in a Pure Oxygen Ambient" Jpn. J. Appl. Phys. **40**, L495 (2001). https://doi.org/10.1143/JJAP.40.L495

[11] C. H. Kuo, S. J. Chang, Y. K. Su, L. W. Wu, J. K. Sheu, C. H. Chen, and G. C. Chi, "Low Temperature Activation of Mg-Doped GaN in O_2 Ambient" Jpn. J. Appl. Phys. **41**, L112 (2002). https://doi.org/10.1143/JJAP.41.L112

[12] W. Götz, N. M. Johnson, J. Walker, D. P. Bour, H. Amano, and I. Akasaki, "Hydrogen passivation

of Mg acceptors in GaN grown by metalorganic chemical vapor deposition" Appl. Phys. Lett. **67**, 2666 (1995). https://doi.org/10.1063/1.114330

[13] A. Castiglia, J.-F. Carlin, and N. Grandjean, "Role of stable and metastable Mg–H complexes in *p*-type GaN for cw blue laser diodes" Appl. Phys. Lett. **98**, 213505 (2011). https://doi.org/10.1063/1.3593964

[14] W. Li, K. Nomoto, K. Lee, S. M. Islam, Z. Hu, M. Zhu, X. Gao, J. Xie, M. Pilla, D. Jena, and H. G. Xing, "Activation of buried p-GaN in MOCVD-regrown vertical structures" Appl. Phys. Lett. **113**, 062105 (2018). https://doi.org/10.1063/1.5041879

[15] S. Usami, R. Miyagoshi, A. Tanaka, K. Nagamatsu, M. Kushimoto, M. Deki, S. Nitta, Y. Honda, and H. Amano, "Effect of dislocations on the growth of p-type GaN and on the characteristics of p–n diodes" Phys. Status Solidi A **214**, 1600837 (2017). https://doi.org/10.1002/pssa.201600837

[16] A. Kumar, K. Mitsuishi, T. Hara, K. Kimoto, Y. Irokawa, T. Nabatame, S. Takashima, K. Ueno, M. Edo, and Y. Koide, "Comparative Analysis of Defects in Mg-Implanted and Mg-Doped GaN Layers on Freestanding GaN Substrates" Nanoscale Res. Lett. **13**, 403 (2018). https://doi.org/10.1186/s11671-018-2804-y

[17] P. P. Michałowski, S. Złotnik, J. Sitek, K. Rosinski, and M. Rudzinski, "Oxygen-induced high diffusion rate of magnesium dopants in GaN/AlGaN based UV LED heterostructures" Phys. Chem. Chem. Phys. **20**, 13890 (2018). https://doi.org/10.1039/C8CP01470A

[18] J.-K. Ho, C.-S. Jong, C. C. Chiu, C.-N. Huang, K. K. Shih, L. C. Chen, F. R. Chen, and J. J. Kai, "Low-resistance ohmic contacts to p-type GaN achieved by the oxidation of Ni/Au films" J. Appl. Phys. **86**, 4491 (1999). https://doi.org/10.1063/1.371392

[19] Y. Koide, T. Maeda, T. Kawakami, S. Fujita, T. Uemura, N. Shibata, and M. Murakami, "Effects of annealing in an oxygen ambient on electrical properties of ohmic contacts to p-type GaN" J. Electron. Mater. **28**, 341 (1999). https://doi.org/10.1007/s11664-999-0037-7

[20] M. Schaffer, B. Schaffer and Q. Ramasse "Sample preparation for atomic-resolution STEM at low voltages by FIB" Ultramicroscopy 114, 62 (2012). https://doi.org/10.1016/j.ultramic.2012.01.005

[21] P. Kozodoy, H. Xing, S. P. DenBaars, U. K. Mishra, A. Saxler, R. Perrin, S. Elhamri, and W. C. Mitchel, "Heavy doping effects in Mg-doped GaN" J. Appl. Phys. **87**, 1832 (2000). https://doi.org/10.1063/1.372098

[22] P. Vennégues. M. Benaissa, B. Beaumont, E. Feltin, P. De Mierry, S. Dalmasso, M. Leroux, and P. Gibart, "Pyramidal defects in metalorganic vapor phase epitaxial Mg doped GaN" Appl. Phys. Lett. **77**, 880 (2000). https://doi.org/10.1063/1.1306421

[23] A. Kumar, J. Uzuhashi, T. Ohkubo, R. Tanaka, S. Takashima, M. Edo and K. Hono, "Atomic-scale quantitative analysis of implanted Mg in annealed GaN layers on free-standing GaN substrates" J. Appl. Phys. **126**, 235704 (2019). https://doi.org/10.1063/1.5132345

[24] A. Kumar, W. Yi, J. Uzuhashi, T. Ohkubo, J. Chen, T. Sekiguchi, R. Tanaka, S. Takashima, M. Edo

and K. Hono “Influence of implanted Mg concentration on defects and Mg distribution in GaN” J. Appl. Phys. **128**, 065701 (2020). https://doi.org/10.1063/5.0014717

[25] J. Uzuhashi, J. Chen, A. Kumar, W. Yi, T. Ohkubo, R. Tanaka, S. Takashima, M. Edo, K. Sierakowski, M. Bockowski, H. Sakurai, T. Kachi, T. Sekiguchi, and K. Hono, J. Appl. Phys. **131**, 185701 (2022). https://doi.org/10.1063/5.0087248

[26] E. Kano, K. Kataoka, J. Uzuhashi, K. Chokawa, H. Sakurai, A. Uedono, T. Narita, K. Sierakowski, M. Bockowski, R. Otsuki, K. Kobayashi, Y. Itoh, M. Nagao, T. Ohkubo, K. Hono, J. Suda, T. Kachi, N. Ikarashi “Atomic resolution analysis of extended defects and Mg agglomeration in Mg-ion-implanted GaN and their impacts on acceptor formation” J. Appl. Phys. **132**, 065703 (2022). https://doi.org/10.1063/5.0097866

[27] L. T. Romano, M. Kneissl, J. E. Northrup, C. G. Van de Walle, and D. W. Treat, “Influence of microstructure on the carrier concentration of Mg-doped GaN films” Appl. Phys. Lett. **79**, 2734 (2001). https://doi.org/10.1063/1.1413222

[28] H. Obloh, K.H. Bachem, U. Kaufmann, M. Kunzer, M. Maier, A. Ramakrishnan, and P. Schlotter, “Self-compensation in Mg doped p-type GaN grown by MOCVD” J. Cryst. Growth **195**, 270 (1998). https://doi.org/10.1016/S0022-0248(98)00578-8

[29] O. Gelhausen, M. R. Phillips, E. M. Goldys, T. Paskova, B. Monemar, M. Strassburg, and A. Hoffmann, “Dissociation of H-related defect complexes in Mg-doped GaN” Phys. Rev. B **69**, 125210 (2004). https://doi.org/10.1103/PhysRevB.69.125210

[30] A. Kumar, W. Yi, T. Ohkubo, J. Chen, T. Sekiguchi, R. Tanaka, S. Takashima, M. Edo and K. Hono “Impact of high-temperature Mg-implantation on defects and dopants distribution in GaN” J. Appl. Phys. 133, 185702 (2023). https://doi.org/10.1063/5.0142766

[31] L. Amichi, I. Mouton, V. Boureau, E. D. Russo, P. Vennéguès, P. D. Mierry, A. Grenier, P.-H. Jouneau, C. Bougero and D. Cooper “Correlative investigation of Mg doping in GaN layers grown at different temperatures by atom probe tomography and off-axis electron holography” Nanotechnology **31,** 045702 (2019). https://doi.org/10.1088/1361-6528/ab4a46

[32] W. Yi, A. Kumar, J. Uzuhashi, T. Kimura, R. Tanaka, S. Takashima, M. Edo, Y. Yao, Y. Ishikawa, J. Chen, T. Ohkubo, T. Sekiguchi, and K. Hono “Mg diffusion and activation along threading dislocations in GaN” Appl. Phys. Lett. **116,** 242103 (2020). https://doi.org/10.1063/5.0009596

[33] D. Iida, K. Tamura, M. Iwaya, S. Kamiyama, H. Amano, and I. Akasaki, “Compensation effect of Mg-doped a- and c-plane GaN films grown by metalorganic vapor phase epitaxy” J. Cryst. Growth **312**, 3131 (2010). https://doi.org/10.1016/j.jcrysgro.2010.07.038

[34] D. D. Koleske, A. E. Wickenden, R. L. Henry, and M. E. Twigg, “Influence of MOVPE growth conditions on carbon and silicon concentrations in GaN” J. Cryst. Growth **342**, 55 (2002). https://doi.org/10.1016/S0022-0248(02)01348-9

[35] A. F. Wright, “Substitutional and interstitial carbon in wurtzite GaN” J. Appl. Phys. **92**, 2575 (2002).

https://doi.org/10.1063/1.1498879

[36] J. Yang, D. G. Zhao, D. S. Jiang, P. Chen, Z. S. Liu, L. C. Le, X. J. Li, X. G. He, J. P. Liu, S. M. Zhang, H. Wang, J. J. Zhu, and H. Yang, "Investigation on the compensation effect of residual carbon impurities in low temperature grown Mg doped GaN films" J. Appl. Phys. **115**, 163704 (2014). https://doi.org/10.1063/1.4873957

[37] H.R. Qi, L.K. Yi, J.L. Huang, S.T. Liu, F. Liang, M. Zhou, D.G. Zhao, and D.S. Jiang, "Compensation of magnesium by residual carbon impurities in p-type GaN grown by MOCVD" J. Alloy. Compd. **765**, 245 (2018). https://doi.org/10.1016/j.jallcom.2018.06.208

[38] C. H. Seager, A. F. Wright, J. Yu, and W. Götz, "Role of carbon in GaN" J. Appl. Phys. **92**, 6553 (2002). https://doi.org/10.1063/1.1518794

[39] R. Niebuhr, K. H. Bachem, U. Kaufmann, M. Maier, C. Merz, B. Santic, P. Schlotter, and H. Jürgensen, "Electrical and optical properties of oxygen doped GaN grown by MOCVD using N_2O" J. Electron. Mater. **26**, 1127 (1997). https://doi.org/10.1007/s11664-997-0007-x .

[40] R.Y. Korotkov and B.W. Wessels, "Electrical Properties of Oxygen Doped GaN Grown by Metalorganic Vapor Phase Epitaxy" MRS Internet J. Nitride Semicond. Res. **5**, 301 (2000). https://doi.org/10.1557/S1092578300004427

[41] J. C. Zolper, R. G. Wilson, S. J. Pearton, and R. A. Stall, "Ca and O ion implantation doping of GaN" Appl. Phys. Lett. **68**, 1945 (1996). https://doi.org/10.1063/1.115634

[42] S. J. Pearton, H. Cho, J. R. LaRoche, F. Ren, R. G. Wilson, and J. W. Lee, "Oxygen diffusion into SiO_2-capped GaN during annealing" Appl. Phys. Lett. **75**, 2939 (1999). https://doi.org/10.1063/1.125194

[43] Ł. Janicki, R. Korbutowicz, M. Rudzinski, P. P. Michałowski, S. Złotnik, M. Grodzicki, S. Gorantla, J. Serafinczuk, D. Hommel, R. Kudrawiec, "Thermal oxidation of [0001] GaN in water vapor compared with dry and wet oxidation: Oxide properties and impact on GaN" Surf Sci. **598**, 153872 (2022). https://doi.org/10.1016/j.apsusc.2022.153872